

Supersymmetric Higgs mediated lepton flavor violation at a Photon Collider

M. CANNONI^{1,2} and O. PANELLA²

¹*Università di Perugia, Dipartimento di Fisica, Via A. Pascoli, I-06123, Perugia, Italy*

²*Istituto Nazionale di Fisica Nucleare, Sezione di Perugia, Via A. Pascoli, 06123 Perugia, Italy*

(Dated: December 15, 2008)

We study a new signature of lepton flavor violation (LFV) at the Photon Collider (PC) within Supersymmetric (SUSY) theories. We consider the minimal supersymmetric standard model within a large $\tan\beta$ scenario with all superpartner masses in the $\mathcal{O}(\text{TeV})$ while the heavy Higgs bosons masses lie below the TeV and develop sizable loop induced LFV couplings to the leptons. We consider a photon collider based on an e^+e^- linear collider with $\sqrt{s} = 800$ GeV with the parameters of the TESLA proposal and show that, with the expected integrated $\gamma\gamma$ -luminosity $L_{\gamma\gamma} = 200 \div 500 \text{ fb}^{-1}$, the “ $\mu\tau$ fusion” mechanism is the dominant channel for the process $\gamma\gamma \rightarrow \mu\tau b\bar{b}$ providing detailed analytical and numerical studies of the signal and backgrounds. We impose on the parameter space present direct and indirect constraints from B physics and rare LFV τ -decays and find that the LFV signal can be probed for masses of the heavy neutral Higgs bosons A, H from 300 GeV up to the kinematical limit $\simeq 600$ GeV for $30 \leq \tan\beta \leq 60$.

PACS numbers: 11.30.Fs, 11.30.Pb, 12.60.Jv, 14.80.Ly, 14.80.Cp

I. INTRODUCTION

There is an emergent consensus in the physics community that the next complementary step to the Cern large hadron collider (LHC) will be the International Linear Collider (ILC) which will collide e^+e^- beams with a center of mass energy in the range $2E_e = 500 - 1000$ GeV [1, 2]. It is also well known, since the pioneering work of the Novosibirsk school, that such a linear collider could offer the possibility of working in the so called $e\gamma$ or $\gamma\gamma$ modes thus realizing a very high energy photon collider (PC) with polarized photon beams [3].

A vast literature is already available on the ILC and the PC potentialities for the discovery and precision measurement of the properties of the Higgs boson, the missing piece of the Standard Model (SM) of electro-weak interactions. Moreover, the properties of extended Higgs sectors of many well motivated theories beyond the SM have been widely considered as well. Among these, the Minimal Supersymmetric Standard Model (MSSM) has received particular attention, for reviews see [4, 5].

However, the MSSM (like the SM) does not provide any explanation for the neutrino masses and mixing. In order to accomplish this task, the seesaw mechanism is usually implemented in the MSSM. Hence we are led to study a MSSM with right handed neutrinos (ν -MSSM). Compared to the MSSM, the main novelty in the ν -MSSM is the presence of lepton flavor violation (LFV). LFV effects arise both in the gauge interactions [6] (through lepton-slepton-gaugino couplings) and in the Yukawa interactions [7]. In particular, LFV Yukawa interactions are greatly enhanced at large $\tan\beta$, and give the possibility of detecting LFV decays of the Higgs bosons at LHC [8, 9] and ILC in the e^+e^- mode [10]. In Refs.[11, 12, 13] loop level lepton flavor violating pro-

cesses such as $e^+e^- \rightarrow e^+\ell^-$ ($\ell = \mu\tau$), and $\gamma\gamma \rightarrow \ell_i\ell_j$ ($\ell_i \neq \ell_j$), which are potentially striking signatures of LFV, were studied in detail.

In this work we extend these previous studies and discuss a new mechanism of lepton flavor violation at the photon collider via the Higgs mediated (H, A) process:

$$\gamma\gamma \rightarrow \mu\tau b\bar{b} \quad (1)$$

in a scenario of large $\tan\beta$ where all the super-partner masses are $\mathcal{O}(\text{TeV})$ and the heavy Higgs bosons (A, H) have instead masses below the TeV and develop sizable loop induced LFV couplings to the SM leptons.

In photon-photon collisions the main production mechanisms for the Higgs bosons are $\gamma\gamma$ fusion [4] (and references therein) and $\tau\tau$ fusion [14]. In the first case, the Higgs is produced as an s-channel resonance through a loop involving the exchange of massive charged particles. In the $\tau\tau$ fusion process $\gamma\gamma \rightarrow \tau\tau b\bar{b}$, the Higgs is produced in the s-channel with a $\tau\tau$ pair and can be detected with its decay mode $b\bar{b}$. We show that the main LFV process is the $\mu\tau$ fusion to the Higgs, see Fig. (1a), which dominate the $\gamma\gamma$ fusion, with large cross section over large portion of the parameter space. The signal from the $\mu\tau$ fusion $\gamma\gamma \rightarrow \mu\tau b\bar{b}$ consists of a $\mu\tau$ pair plus $b\bar{b}$ jets from the Higgs decay, allowing the possibility to detect and reconstruct the Higgs through its main decay channel and to measure, at the same time, the size of LFV couplings. In Ref. [14] it is shown that the lepton flavor conserving (LFC) channel $\gamma\gamma \rightarrow \tau\tau b\bar{b}$ (“ $\tau\tau$ fusion”) allows to measure $\tan\beta$ with a precision which is better than 10% at large $\tan\beta$.

The plan of the paper is the following. In Section II we review the theory of lepton flavor violation related to the MSSM Higgs bosons and discuss their properties within our scenario. Section III is devoted to the analytical evaluation of the signal cross sections at the photon

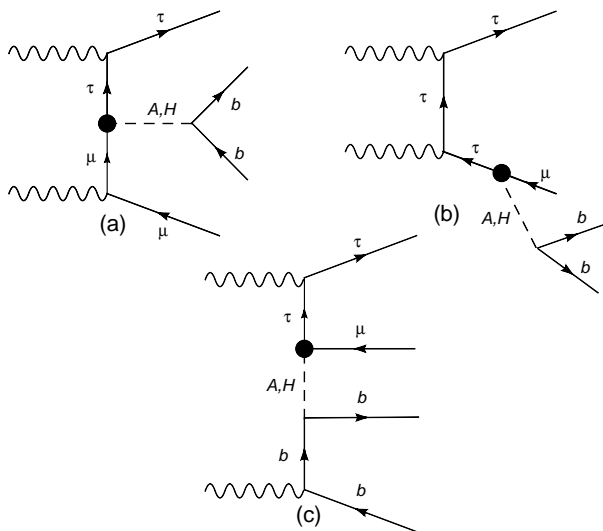


FIG. 1: Diagrams for the process $\gamma\gamma \rightarrow \mu\tau\bar{b}b$: the topology (a) is the one we call $\mu\tau$ fusion. The black blob represents the loop induced LFV coupling treated as an effective vertex.

collider; in Section IV we present numerical simulations of both the signal and the background. The correlations among the signal at the PC and the constraints imposed by B physics and the non observation of SUSY particles and lepton flavor violating rare τ -decays is discussed in Section V. Finally, we give a summary and the conclusions in Section VI.

II. HIGGS LFV IN SUSY

Within a SUSY framework, LFV effects originate from any misalignment between fermion and sfermion mass eigenstates. In particular, if the light neutrino masses are obtained via a see-saw mechanism, the radiatively induced off-diagonal (LFV) entries in the slepton mass matrix $(m_{\tilde{L}}^2)_{ij}$ are given by [6, 15, 16]:

$$(m_{\tilde{L}}^2)_{i\neq j} \approx -\frac{3m_0^2}{8\pi^2}(Y_\nu Y_\nu^\dagger)_{i\neq j} \ln\left(\frac{M_X}{M_R}\right), \quad (2)$$

where M_X denotes the scale of SUSY-breaking mediation, M_R the scale of the heavy right-handed neutrinos masses, m_0 the universal supersymmetry breaking scalar mass and Y_ν the Yukawa couplings between left- and right-handed neutrinos (the potentially large sources of LFV). Since the see-saw equation $m_\nu = -Y_\nu \hat{M}_R^{-1} Y_\nu^T \langle H_u \rangle^2$, with $\langle H_u \rangle$ is the vacuum expectation value of the up-type Higgs, allows large $(Y_\nu Y_\nu^\dagger)$ entries, sizable effects can stem from this running. The determination of $(m_{\tilde{L}}^2)_{i\neq j}$ would imply a complete knowledge of the neutrino Yukawa matrix $(Y_\nu)_{ij}$, which is not possible even if all the low-energy observables from the neutrino sector were known [17]. As a result, the predictions of

leptonic flavor changing neutral current effects will remain undetermined even in the very optimistic situation where all the relevant New Physics masses were measured at the LHC. More stable predictions can be obtained embedding the SUSY model within a Grand Unified Theory (GUT) where the see-saw mechanism can naturally arise (such as $SO(10)$) [18]. In this case the GUT symmetry allows us to obtain some hints about the unknown neutrino Yukawa matrix Y_ν .

There exist two different classes of LFV contributions to rare decays: gauge-mediated LFV effects through the exchange of gauginos and sleptons [6, 15, 16] and Higgs-mediated LFV effects through effective non-holomorphic Yukawa interactions for quarks and leptons [7, 19]: once a source of LFV is given in the slepton mass matrix, for example Eq. (2) in MSSM with the see saw mechanism, LFV Yukawa coupling of the type $\bar{L}_R^i L_L^j H_u^*$ are induced at loop level and become particularly sizable at large $\tan\beta$.

In the mass-eigenstate basis for both leptons and Higgs bosons, the effective flavor-violating Yukawa interactions are described by the lagrangian:

$$\begin{aligned} -\mathcal{L} \simeq & (2G_F^2)^{\frac{1}{4}} \frac{m_{l_i}}{c_\beta} \left(\Delta_L^{ij} \bar{l}_R^i l_L^j + \Delta_R^{ij} \bar{l}_L^i l_R^j \right) \\ & \times (c_{\beta-\alpha} h - s_{\beta-\alpha} H - iA) + h.c. \\ & + (8G_F^2)^{\frac{1}{4}} \frac{m_{l_i}}{c_\beta} \left(\Delta_L^{ij} \bar{l}_R^i \nu_L^j + \Delta_R^{ij} \nu_L^i \bar{l}_R^j \right) H^\pm + h.c. \end{aligned} \quad (3)$$

where α is the mixing angle between the CP-even Higgs bosons h and H , A is the physical CP-odd boson, H^\pm are the physical charged Higgs-bosons and we adopt the notation $(c_\theta, s_\theta, t_\theta) = (\cos\theta, \sin\theta, \tan\theta)$. We note that in Eq. (3) i, j are flavor indices that in the following are understood to be different ($i \neq j$).

In supersymmetry, the couplings Δ^{ij} in Eq. (3) are induced at one loop level by the exchange of gauginos and sleptons, provided a source of slepton mixing is present. In this work the analysis at Higgs LFV effects will be model independent and we use the expressions of $\Delta_{L,R}^{ij}$ obtained in the mass insertion (MI) approximation [21]:

$$\begin{aligned} \Delta_L^{ij} = & -\frac{\alpha_1}{4\pi} \mu M_1 \delta_{LL}^{ij} m_L^2 \\ & \times \left[I'(M_1^2, m_R^2, m_L^2) + \frac{1}{2} I'(M_1^2, \mu^2, m_L^2) \right] \\ & + \frac{3}{2} \frac{\alpha_2}{4\pi} \mu M_2 \delta_{LL}^{ij} m_L^2 I'(M_2^2, \mu^2, m_L^2), \end{aligned} \quad (4)$$

$$\Delta_R^{ij} = \frac{\alpha_1}{4\pi} \mu M_1 m_R^2 \delta_{RR}^{ij} [I'(M_1^2, \mu^2, m_R^2) - (\mu \leftrightarrow m_L)] \quad (5)$$

where μ is the the Higgs mixing parameter, $M_{1,2}$ are the gaugino masses and $m_{L(R)}^2$ stands for the left-left

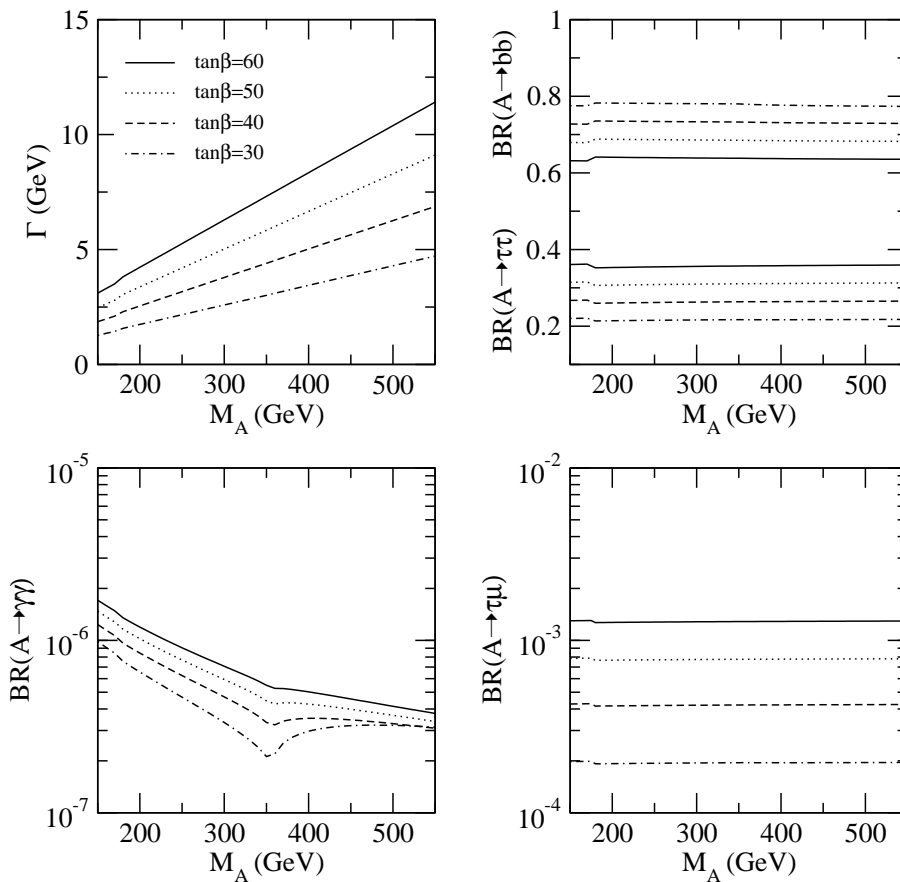


FIG. 2: (Top-left panel) Total width of the A Higgs boson for large values of $\tan\beta$ explained in the legend. (Top-right panel) Branching ratios for the main decay channel $b\bar{b}$ and $\tau^+\tau^-$. (Bottom-left panel) Branching ratio for $\gamma\gamma$ decay. (Bottom-right panel) Branching ratio for the LFV decay $A \rightarrow \mu\tau$. The results are obtained by means of the code FEYNHIGGS [20] and Eq. (11) with SUSY parameters $M_{SUSY} = M_{1,2,3} = 1$ TeV, $\mu = 2$ TeV, $\Delta^2 = |\Delta_L^{32}|^2 + |\Delta_R^{32}|^2 = 10^{-6}$.

(right-right) slepton mass matrix entry. The LFV mass insertions δ_{LL}^{ij} and δ_{RR}^{ij} are defined as:

$$\delta_{LL}^{ij} = \frac{(m_L^2)^{ij}}{m_L^2}, \quad \delta_{RR}^{ij} = \frac{(m_R^2)^{ij}}{m_R^2}, \quad (6)$$

where $(m_L^2)^{ij}$ are the off-diagonal flavor changing entries of the slepton mass matrix. Let us emphasize that the parameters δ_{LL}^{ij} and δ_{RR}^{ij} will be treated in the following study as free parameters in order to provide a model independent study of LFV signals. The loop function I' is defined by $I'(x, y, z) = dI(x, y, z)/dz$, where $I(x, y, z)$ is the three point one-loop integral

$$I(x, y, z) = \frac{xy \log(x/y) + yz \log(y/z) + zx \log(z/x)}{(x-y)(z-y)(z-x)}. \quad (7)$$

While gaugino mediated lepton flavor violation decouples with the heaviest mass in the slepton/gaugino loops m_{SUSY} , Higgs mediated effects of LFV do not decouple increasing the sparticles masses because Δ_L , Δ_R , which appear in the couplings of the dimension-four lagrangian (Eq. 3), are dimensionless coefficients given by

ratios of SUSY masses. Higgs mediated effects in rare decays start being competitive with the gaugino mediated ones when m_{SUSY} is roughly one order of magnitude heavier than m_H and for large $\tan\beta$. Phenomenological analysis of rare LFV τ decays and B meson decays have been widely discussed in the recent literature [7, 19, 21, 22, 23, 24, 25, 26, 27, 28, 29, 30, 31].

The Higgs boson decay widths and branching ratios are obtained by means of the lagrangian of Eq. (3) using the approximation $1/c_\beta^2 \simeq \tan^2\beta$ (only valid in the large $\tan\beta$ regime) and in the limit of massless fermions. Introducing $\Delta^2 = |\Delta_L^{32}|^2 + |\Delta_R^{32}|^2$ we find:

$$\Gamma(A \rightarrow \tau^+\mu^-) = \frac{1}{8\pi} \frac{m_\tau^2}{v^2} M_A t_\beta^4 \frac{\Delta^2}{2}. \quad (8)$$

where $v = (v_u^2 + v_d^2)^{1/2} \approx 246$ GeV, v_u and v_d being the expectation values of the Higgs fields H_u and H_d . The width for the lepton flavor conserving decay to $\tau^+\tau^-$ pair

is, with the same approximations:

$$\Gamma(A \rightarrow \tau^+ \tau^-) = \frac{1}{8\pi} \frac{m_\tau^2}{v^2} M_A t_\beta^2, \quad (9)$$

and therefore:

$$\Gamma(A \rightarrow \tau^+ \mu^-) = \frac{1}{2} t_\beta^2 \Delta^2 \Gamma(A \rightarrow \tau^+ \tau^-). \quad (10)$$

Finally since $\Gamma(A \rightarrow \tau^+ \mu^-) = \Gamma(A \rightarrow \tau^- \mu^+)$ we find also:

$$\Gamma(A \rightarrow \tau^+ \mu^-) + \Gamma(A \rightarrow \tau^- \mu^+) = t_\beta^2 \Delta^2 \Gamma(A \rightarrow \tau^+ \tau^-),$$

$$\mathcal{B}(A \rightarrow \mu^+ \tau^-) + \mathcal{B}(A \rightarrow \mu^- \tau^+) = t_\beta^2 \Delta^2 \mathcal{B}(A \rightarrow \tau^+ \tau^-). \quad (11)$$

For the heavy higgs boson H , the right hand sides of Eq. (11), should be multiplied by a factor $(s_{\beta-\alpha}/c_\alpha)^2$. Let us remark that the light Higgs field h has negligible lepton flavor violating decays since its coupling $\cos(\beta - \alpha) \rightarrow 0$ in the decoupling regime. In Fig. 2 we show $\mathcal{B}(A \rightarrow b\bar{b})$ and $\mathcal{B}(A \rightarrow \gamma\gamma)$ for different values of $\tan\beta$ and for the reference point of the parameter space $M_{SUSY} = M_{1,2,3} = 1$ TeV, $\mu = 2$ TeV. For completeness, in Fig. 2 we also report the absolute value of the total width Γ_A and the branching ratio for the LFV decay $A \rightarrow \mu\tau$ given by Eq. (11) with $\Delta^2 = 10^{-6}$.¹ We note the following features: *i*) the total width is of the order of a few GeV, comparable, but always smaller, than the expected resolution of the invariant mass of the $b\bar{b}$ system (see Section IV); *ii*) the total decay width is saturated almost exactly by the two decays $A \rightarrow b\bar{b}$ and $A \rightarrow \tau\tau$ while $A \rightarrow \gamma\gamma$ is strongly suppressed; *iii*) finally the branching ratio $\mathcal{B}(A \rightarrow \mu\tau)$ is in the interesting region of $10^{-4} \div 10^{-3}$.

III. HIGGS LFV AT A PHOTON COLLIDER

High-energy photon beams [2, 3] will be obtained from Compton back-scattered (CB) low-energy laser photons with energy ω_0 off high-energy electron beams with energy E_e . These high-energy photon beams will not be monochromatic but will present instead an energy spectrum, mainly determined by the Compton cross section. The spectrum of the fraction of the electron's energy retained by the photon have a maximum at $E_{max}^\gamma = y_{max} E_e$, where $y_{max} = x/(x+1)$ with $x = 4E_e \omega_0 / m_e^2$. As a consequence, if y_1 and y_2 are the fractions of energies of the colliding photons, the number of photon collisions as a function of the invariant mass $W_{\gamma\gamma} = y_1 y_2 2E_e$

will present a spectrum too. In first approximation, the luminosity spectrum is given by the convolution of two Compton cross-sections, that is

$$\frac{dL_{\gamma\gamma}^{CB}}{dz} = 2z \int_{-\ln y_m/z}^{\ln y_m/z} F_c(x, ze^{+\eta}) F_c(x, ze^{-\eta}) d\eta, \quad (12)$$

where we introduce the variables $z = \sqrt{y_1 y_2} = W_{\gamma\gamma}/2E_e = \sqrt{s_{\gamma\gamma}/s_{ee}}$, $\eta = \ln \sqrt{y_1/y_2}$ and F_c is the Compton cross section; thus $s_{\gamma\gamma} = z^2 s_{ee}$ with $s_{ee} = (2E_e)^2$. Even if the simulated realistic differential spectrum as a function of z cannot be described analytically, the luminosity peak near z_{max} is almost independent from the details of the machine, and is well described by Eq. (12). We consider a PC taking the parameters of TESLA(800): $2E_e = 800$ GeV, $x = 5.2$. $2E_\gamma$ in the region of the peak covers the range 535 – 670 GeV, and the corresponding photon-photon luminosity at the peak is $L_{\gamma\gamma}(z > 0.8z_m) = 1.7 \times 10^{34} \text{ cm}^{-2} \text{ s}^{-1} \simeq 500 \text{ fb}^{-1} \text{ yr}^{-1}$. To use these numbers as representative of the PC luminosity, we follow the approach of Ref. [12], in which the ideal spectrum, Eq. (12), is normalized in the following way:

$$\frac{dL_{\gamma\gamma}^{norm}}{dz} = \frac{1}{\int_{0.8z_{max}}^{z_{max}} dz \frac{dL_{\gamma\gamma}^{CB}}{dz}} \frac{dL_{\gamma\gamma}^{CB}}{dz}, \quad (13)$$

Defining the effective cross section as:

$$\sigma^{eff} = \int_{z_{min}}^{z_{max}} dz \frac{dL_{\gamma\gamma}^{norm}}{dz} \sigma(W_{\gamma\gamma}), \quad (14)$$

the total number of events can be evaluated to be $N_{events} = L_{\gamma\gamma} \times \sigma^{eff}$, where $L_{\gamma\gamma}$ is the simulated TESLA luminosity at the peak.

In photon-photon collisions the main production mechanisms for the Higgs bosons are $\gamma\gamma$ fusion [4] and $\tau\tau$ fusion [14]. In the first the Higgs is produced as an s-channel resonance through a loop involving the exchange of all charged massive particles. This process is particularly well suited for precision studies of the Higgs sector when the mass(es) of the Higgs boson(s) is (are) known, given that the width of the decay into two photons (which controls the production cross section) is not too small. Assuming that the machine energy could be tuned to the Higgs mass then one could take advantage of the resonant production in order to probe the details of the Higgs sector. However in the case of $\tan\beta$ enhanced Higgs-lepton coupling the $\tau\tau$ fusion becomes competitive or even dominant over a wider range of masses. In order to appreciate the differences between the two mechanisms, we first give analytical expressions of the cross sections for the LFV Higgs mediated signals and then make numerical estimates. For clarity, we fix the following SUSY parameters to: $M_{SUSY} = M_{1,2,3} = 1$ TeV, $\mu = 2$ TeV, $\tan\beta = 50$, $\Delta^2 = |\Delta_L^{32}|^2 + |\Delta_R^{32}|^2 = 10^{-6}$, as for the calculation reported in Figure 2; the widths and branching

¹ We note that our formula in Eq. (8) agrees with the corresponding formulas in Ref. [26, 32], but we find a disagreement by a factor 1/2 with that in [8, 9].

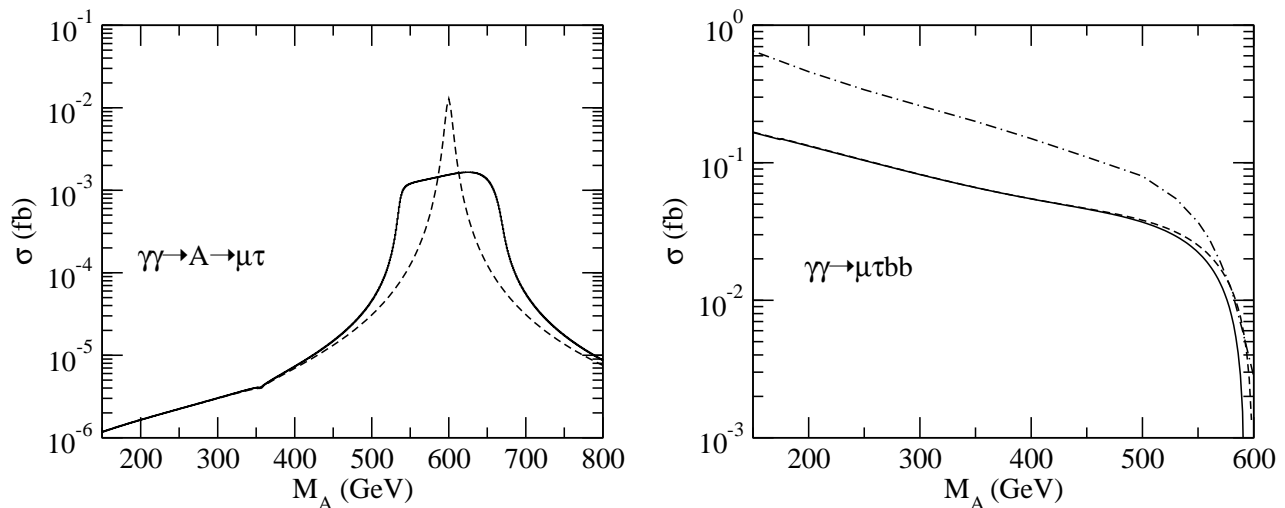


FIG. 3: (Left panel) Cross section for $\gamma\gamma \rightarrow A \rightarrow \mu\tau$ as a function of M_A : dashed line monochromatic photons, in full line the effective cross section with photons luminosity. (Right panel) Cross section for $\gamma\gamma \rightarrow \mu\tau b\bar{b}$. Full line: monochromatic photons and equivalent particle approximation plus small width approximation, Eq. (18). Dashed line: effective cross section, Eq. (19). Dot-dashed line: exact result by COMPHEP. The relevant parameters are $\tan\beta = 50$, $|\Delta_L^{32}|^2 + |\Delta_R^{32}|^2 = 10^{-6}$, $M_{SUSY} = M_{1,2,3} = 1$ TeV, $\mu = 2$ TeV.

ratios which appear in the following formulas are computed with the software FEYNHIGGS [20] linked to our own code.

The cross section for the resonant process $\gamma\gamma \rightarrow A \rightarrow \mu\tau$ in the monochromatic case is provided by a Breit-Wigner formula [4]:

$$\sigma(s_{\gamma\gamma}) = 8\pi \frac{\Gamma(A \rightarrow \gamma\gamma) \Gamma(A \rightarrow \tau\mu)}{(s_{\gamma\gamma} - M_A^2)^2 + (\Gamma_A M_A)^2} (1 + \lambda_1 \lambda_2) \quad (15)$$

where $\lambda_{1,2}$ are the photons helicities and we take $\lambda_1 \lambda_2 = 1$. The effective cross section is obtained by folding Eq.(15) in Eq. (14). In Fig. 3 we plot with a dashed line the monochromatic cross section with $2E_\gamma = 600$ GeV and with a full line the effective cross section with $2E_e = 800$ GeV: the resonance peak at $M_A = 600$ GeV is only smoothed by the effect of the photon spectra, while it is clear that in mass regions away from the resonance the effect of the photon spectra is totally negligible. Even if the resonant effect is evident around $M_A = 600$ GeV, the cross section is rather small, at the level $10^{-2} \div 10^{-3}$ fb, being suppressed by $\Gamma(A \rightarrow \gamma\gamma)$ which in our scenario is $\mathcal{O}(10^{-6})$ GeV, as can be seen in Fig. 2.

The $\mu\tau$ fusion process $\gamma\gamma \rightarrow \mu\tau b\bar{b}$ corresponds to the diagram (a) in Fig. 1. Here the Higgs boson is produced in the s-channel via a virtual $\mu\tau$ pair and can be detected from its decay mode $A \rightarrow b\bar{b}$. The black blob in the vertex of the diagram represents the loop induced LFV coupling. A first estimate of the production cross section can be obtained using the equivalent particle approximation (EPA) wherein the colliding real photons split into τ and μ pairs with the subsequent $\mu\tau$ fusion into the Higgs boson. Following Ref. [14], we introduce

the photon splitting function into a pair of leptons

$$P_{\gamma/\ell}(x) = \frac{\alpha}{2\pi} [x^2 + (1-x)^2] \ln\left(\frac{\mu_F^2}{m_\ell^2}\right) \quad (16)$$

where x is the fraction of the energy of the photon carried by the virtual lepton and μ_F is the factorization scale that we set to $\mu_F = M_A$. The on shell $\mu\tau \rightarrow b\bar{b}$ fusion cross section in the center of mass frame is easily calculated from the lagrangian of Eq. (3) and expressed in terms of the partial widths given in Section II:

$$\sigma(\hat{s}) = \frac{4\pi\Gamma(A \rightarrow \tau\mu)\Gamma(A \rightarrow b\bar{b})\hat{s}}{M_A^2(\hat{s} - M_A^2)^2 + (\Gamma_A M_A)^2}. \quad (17)$$

where \hat{s} is $\mu\tau$ center of mass energy squared. The cross section for monochromatic photons is given by the convolution of Eq. (17) with the splitting functions,

$$\sigma(\gamma\gamma \rightarrow \mu\tau b\bar{b}; s_{\gamma\gamma}) = 2 \int dx_\mu dx_\tau P_{\gamma/\mu}(x_\mu) P_{\gamma/\tau}(x_\tau) \sigma(\hat{s}),$$

where $s_{\gamma\gamma}$ is the center of mass energy squared of the photons which is related to \hat{s} by $\hat{s} = x_\mu x_\tau s_{\gamma\gamma}$ and the factor two is the multiplicity factor which accounts for the exchange of the initial photons. The formula is simplified by changing the integration variables (x_μ, x_τ) to (η, \hat{s}) with $\eta = \ln \sqrt{x_\mu/x_\tau}$ and using the small width approximation (SWA) when performing the integration over \hat{s} . The result is:

$$\begin{aligned} \sigma(\gamma\gamma \rightarrow \mu\tau b\bar{b}; s_{\gamma\gamma}) &= \frac{4\pi^2 \Gamma(A \rightarrow \tau\mu) \mathcal{B}(A \rightarrow b\bar{b})}{s_{\gamma\gamma} M_A} \\ &\times 2 \int_{-\ln 1/t}^{+\ln 1/t} d\eta P_{\gamma/\mu}(te^\eta) P_{\gamma/\tau}(te^{-\eta}). \end{aligned} \quad (18)$$

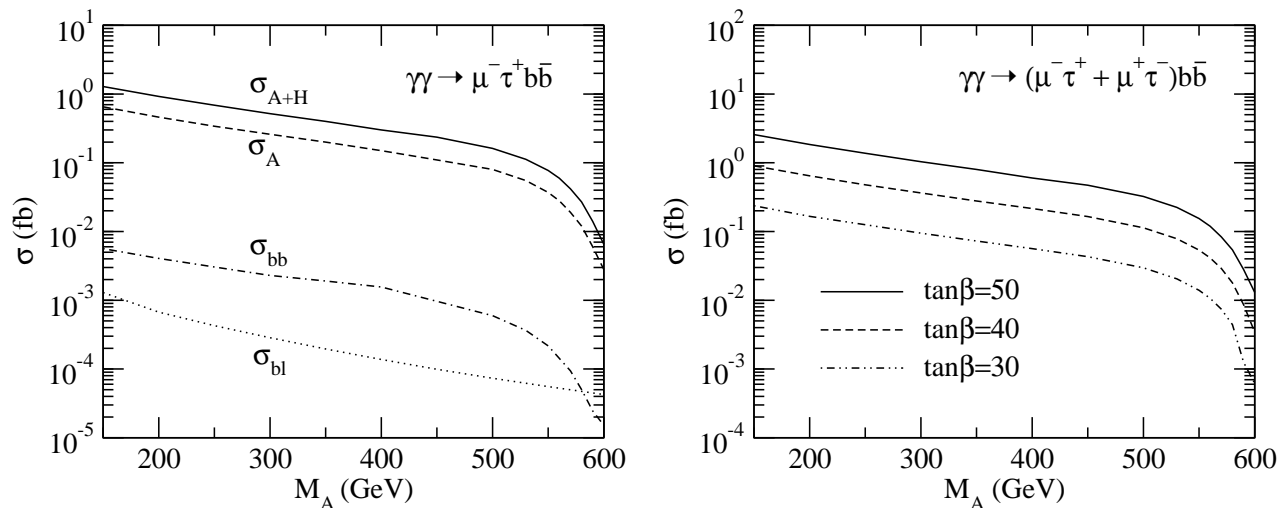


FIG. 4: (Left-panel) Total cross for $\gamma\gamma \rightarrow \mu\tau b\bar{b}$ with monochromatic photons at $2E_\gamma = 600$ GeV as a function of M_A and $\tan\beta = 50$. Full line: all contributing diagrams with A and H . Dashed line: only diagrams with A . Dot-dashed line: $b\bar{b}$ fusion cross section. Dotted line: contribution of the peripheral diagrams. (Right panel) Exact cross section with A and H diagrams for different values of the $\tan\beta$. The other parameters are the same as in Fig. (3).

with $t = M_A/2E_\gamma$. Finally, the effective cross section is obtained by the convolution of Eq. (18) with the photon spectra; defining $t = M_A/2E_e$ we have

$$\begin{aligned} \sigma_{eff} = & \frac{4\pi^2 \Gamma(A \rightarrow \tau\mu)\mathcal{B}(A \rightarrow b\bar{b})}{s_{ee} M_A} \\ & \times \left[\int_{z_{min}}^{z_{max}} dz \frac{dL_{\gamma\gamma}^{norm}}{dz} \right. \\ & \left. \times 2 \int_{-\ln 1/zt'}^{+\ln 1/zt'} d\eta P_{\gamma/\mu} \left(\frac{t'}{z} e^\eta \right) P_{\gamma/\tau} \left(\frac{t'}{z} e^{-\eta} \right) \right] \end{aligned} \quad (19)$$

In Fig. 3 we plot the Eq. (18) and Eq. (19) as functions of M_A . The cross section is in the range $10^{-2} - 1$ fb in the range of Higgs masses $100 - 550$ GeV, thus dominant respect to the $\gamma\gamma$ fusion one. Moreover, the use of the photon luminosity spectrum with $2E_e = 800$ GeV and $x = 5.2$ gives the same numerical results for the cross section calculated with monochromatic photons with $2E_\gamma = 600$ GeV which represents the value of the mean energy at the luminosity peak, $535 \text{ GeV} \leq 2E_\gamma \leq 670 \text{ GeV}$, so that from now on we consider this situation of monochromatic photon beams to simplify the calculations.

To estimate the accuracy of the analytical formulas we also show in Figure 3 (right plot) the cross section calculated with Eq. (18) and the one calculated with the program COMPHEP [33] in which we have implemented the MSSM with LFV as described by the lagrangian in Eq. (3). The dotted dashed curve is obtained considering the $\mu\tau$ fusion diagrams and bremsstrahlung diagrams with the A boson contribution, Figure 1(a-b), which, as we show explicitly in Section IV, are the dominant dia-

grams. The analytical result gives the correct order of magnitude of the cross section, but for low Higgs masses it underestimates the exact result by a factor 3–5, and only for masses approaching to $2E_\gamma$, the kinematical limit, the approximation is better. This analytical study served us to provide a preliminary evaluation of the orders of magnitude of the signal and to understand the dominant mechanisms involved. In the following Section IV we present the results of full numerical tree-level simulations obtained by means of COMPHEP.

IV. SIGNAL AND BACKGROUND

The process $\gamma\gamma \rightarrow \mu\tau b\bar{b}$ mediated by the heavy Higgs bosons A and H is described by a set of 40 diagrams which can be classified by the three topologies depicted in Figure 1: (a) the $\mu\tau$ fusion diagrams where the Higgs is in the s channel; (b) bremsstrahlung diagrams, where the Higgs is radiated by a lepton of an external leg; (c) peripheral diagrams, where the Higgs bosons are exchanged in the $t - (u)$ channel. In our numerical calculations we have divided them into three groups: (group-1) 12 diagrams (topology (a) and (b)) describe what we call “ $\mu\tau$ fusion” to A, H ; (group-2) 12 diagrams which describe “ $b\bar{b}$ fusion” to A, H (the are given by the topologies (a) and (b) of Fig. 1 with the role of $\mu\tau$ and $b\bar{b}$ excahnged); (group-3) 26 diagrams of topology (c) that we call “ bl fusion”.

In Figure 4, left panel, we plot the contribution to the total cross section of these groups, $\sigma_{\mu\tau}$, σ_{bb} and σ_{bl} , respectively. We observe the following features: σ_{bb} , even if it is described by diagrams with the same phase-space

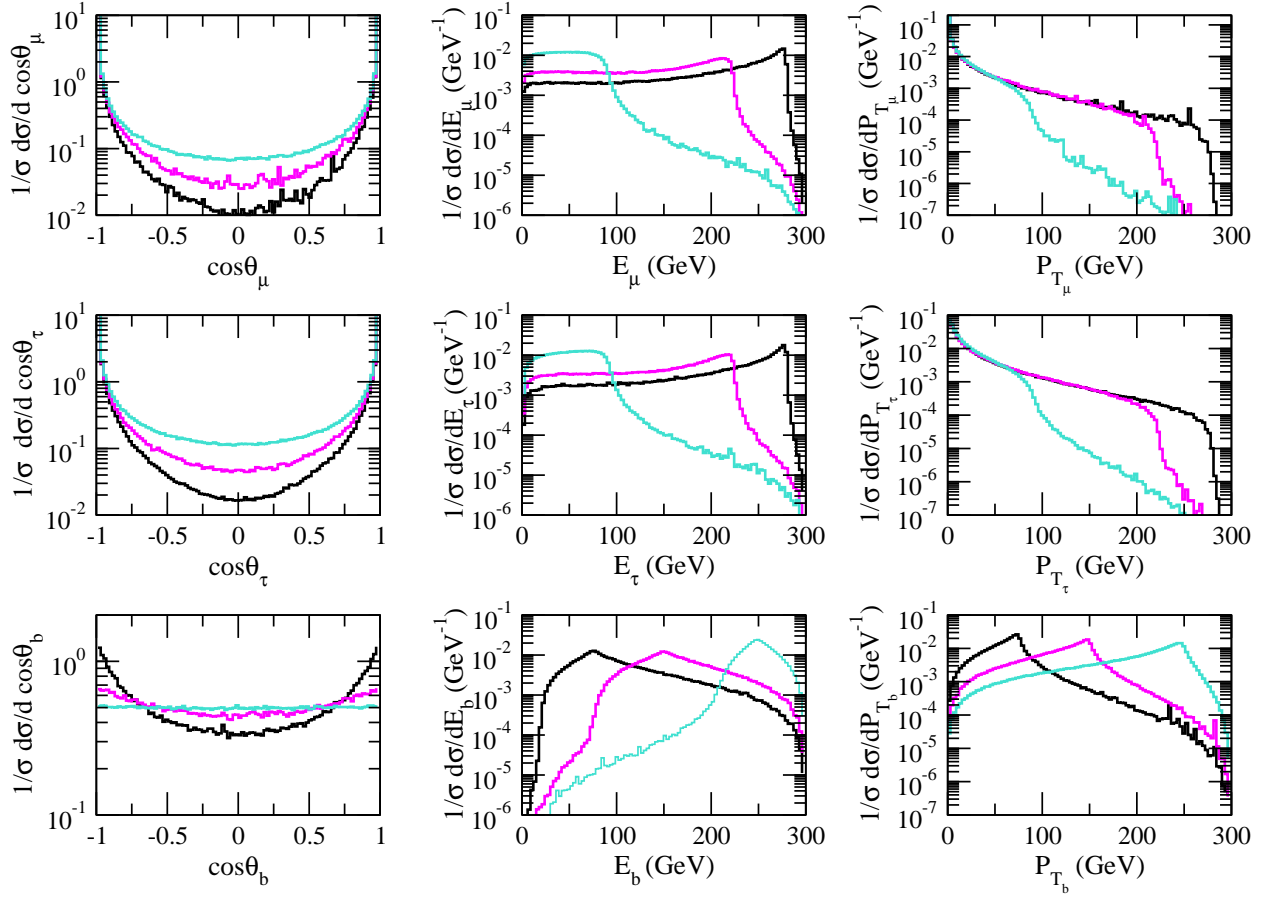


FIG. 5: (Left column) Distributions for scattering angle respect the collision axis for leptons and jets. (Central column) Distributions for the energy of leptons and jets. (Right column) Distributions for the transverse momentum of leptons and jets. Black line: $M_{A,H} = 150$ GeV, Magenta: $M_{A,H} = 300$ GeV, Cyan: $M_{A,H} = 500$ GeV. The other parameters are the same of Figs. (3).

structure of $\sigma_{\mu\tau}$, is two orders of magnitude smaller because those diagrams with two b -quark attached to photon lines bring in a charge factor of $(1/3)^2$ in the amplitude; σ_{bl} is three orders of magnitude smaller of $\sigma_{\mu\tau}$, both for the presence in the diagrams of at least one $bb\gamma$ coupling and the absence of s -channel resonant propagators; finally we note that in $\sigma_{\mu\tau}$ the contributions of diagrams with A and H sum up incoherently, i.e. their interference vanishes. Since in the limit of large $\tan\beta$, $M_A \approx M_H$ and also the couplings of the higgs bosons A and H become approximatively equal we have $\sigma_{A+H} \approx 2\sigma_A$. We conclude that the signal cross section is completely determined by $\sigma_{\mu\tau}$, while σ_{bb} and σ_{bl} , which are irreducible backgrounds are negligible. (We also checked that the interference of these subleading contributions with the dominant one is negligible.)

The right panel of Figure 4 shows the total cross section $\sigma_{\mu\tau}$ for $\tan\beta$ in the range $30 < \tan\beta < 50$ as a function of M_A ; a factor of two as been included to account for the charged conjugated process which has the same total cross section. With $\Delta^2 = |\Delta_L|^2 + |\Delta_R|^2 = 10^{-6}$

the cross sections range from 10^{-2} fb to 2 fb with M_A ranging from 150 GeV to ≈ 550 GeV. Assuming an integrated luminosity for the photon collider in the range $200 - 500 \text{ fb}^{-1}/\text{yr}$, a relatively large number of events are thus predicted, from $N_{events} \approx 200 - 500$ for $M_A = 100$ GeV down to $N_{events} \approx 20 - 50$ when $M_A \approx 550$ GeV. However, we show in the next section, that these numbers are rather optimistic. The results on the collider cross sections must be correlated with the constraints on the Susy spectrum, B -physics and LFV τ decays are considered. Once this is done the allowed parameter space is reduced and more realistic predictions emerge.

In Fig. 5, left column, are shown the angular distributions as function of the cosine of the angle between one particle (μ, τ, jet) with the positive direction of the collision axis for three values of $M_{A,H} = (150, 300, 500)$ GeV. The distribution is peaked along the collision axis for the leptons and the effect is more pronounced at low Higgs masses, while for jets the cross cross section is less concentrated in the forward-backward directions and is practically flat for $M_{A,H}$ above 300 GeV. The distributions in

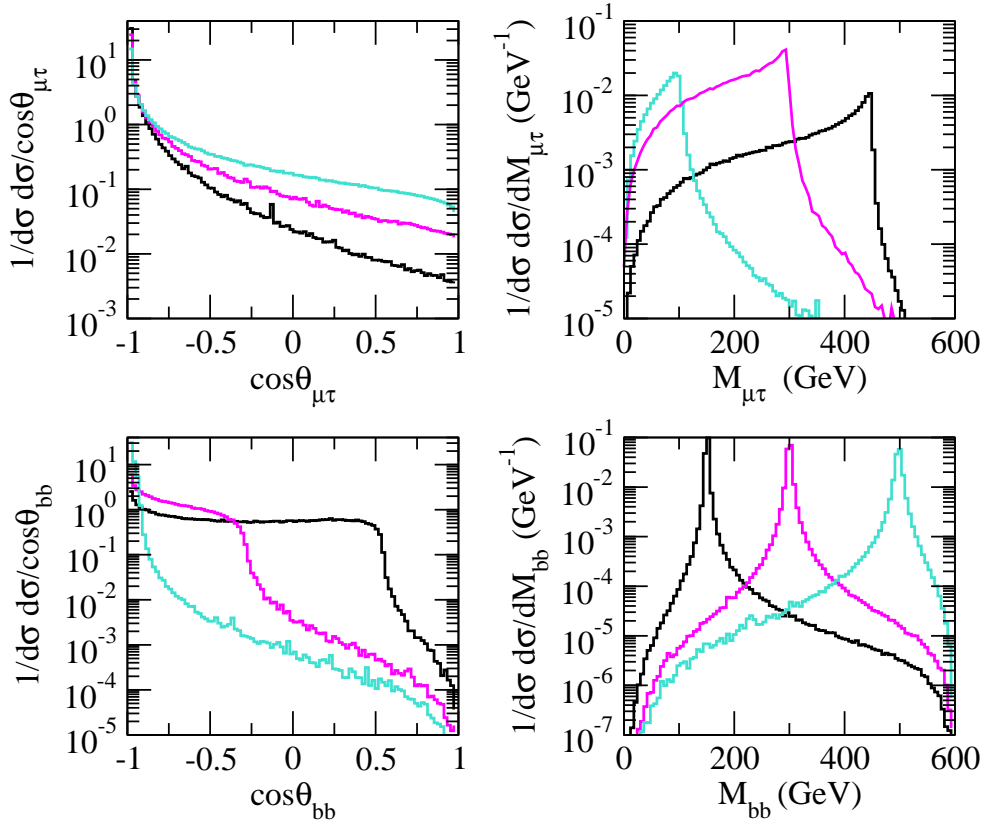


FIG. 6: (Left column) Distributions for opening angle between the two leptons and the jets. (Right column) Distributions for the invariant mass of leptons pair and $b\bar{b}$. Black line: $M_{A,H} = 150$ GeV, Magenta: $M_{A,H} = 300$ GeV, Cyan: $M_{A,H} = 500$ GeV. The other parameters are the same of Fig. (3).

the transverse momentum (right column) are consistent with the angular distributions, leptons have low p_T , the quarks have high transverse momentum with distribution peaked around $M_{A,H}/2$. For the b-jets also the energy distribution (central column) is peaked at $M_{A,H}/2$, while leptons are more energetic for low Higgs masses. Other interesting features of the signal are given by the distribution for the cosine of the angle between the leptons and jets shown in Fig. 6, left column. Both are peaked towards $\cos\theta_{ij} \rightarrow -1$, thus both the lepton pair and the jet pair will be well separated being almost back-to-back, the effect being stronger for the b-tagged jets at high $M_{A,H}$. On the right column, we plot the invariant mass distribution for $\mu\tau$ pair and the $b\bar{b}$ pair: while the former extends up to $\sqrt{s_{\gamma\gamma}} - M_{A,H}$, the latter has a peak at the Higgs mass, as expected, because of the s-channel propagator in the amplitude. Thus the signal has the following characteristics: the Higgs decay to a pair of back to back b-jets with energy and transverse momentum around $M_A/2$ and invariant mass peaked at M_A . The μ and the τ are also back to back and in forward-backward directions with low P_T .

The background processes from the SM are the ones with the final state $\mu\tau b\bar{b}$ +neutrinos. The main processes

are:

$$\begin{aligned} (a) & \gamma\gamma \rightarrow Z^*Z^* \rightarrow (b\bar{b})(\tau^+\tau^{*-}) \rightarrow b\bar{b}\tau^+\mu^-\bar{\nu}_\mu\nu_\tau \\ (b) & \gamma\gamma \rightarrow W^{*+}W^{*-}Z^*(\gamma^*) \rightarrow (\tau^+\nu_\tau)(\mu^-\bar{\nu}_\mu)(b\bar{b}). \end{aligned}$$

The cross sections for double and triple gauge boson production are known to be large in photon-photon collisions [2]. At $\sqrt{s_{\gamma\gamma}} = 600$ GeV they are: $\sigma(\gamma\gamma \rightarrow ZZ) = 0.2$ pb and $\sigma(\gamma\gamma \rightarrow WWZ) = 0.7$ pb. We estimate the cross section for the complete processes by multiplying the above numbers by the appropriate branching ratios for the decay chains and find: $\sigma_a \simeq 1.77 \times 10^{-1}$ fb and $\sigma_b \simeq 1.26$ fb. The jets coming from Z decay have very different distributions and energies from those of the jets from Higgs decay. Moreover, while the signal has no missing energy or missing transverse momentum, the two neutrinos in the final state of the SM backgrounds carry away a large fraction of the energy/momentum, thus providing large missing energy and momentum.

As the bulk of the cross section is determined by those regions of phase space where the leptons are emitted with small angle and low transverse momenta and therefore might escape detection, it is essential to evaluate the expected number of events including angular cuts. We apply a cut of $\theta > 130$ mrad on the scattering angles

TABLE I: Effect of cuts on the cross section for $\gamma\gamma \rightarrow \mu\tau b\bar{b}$: σ^{cut} is obtained imposing for all particles in the final state: scattering angle $\theta > 130$ mrad, $E > 5$ GeV, $b\bar{b}$ invariant mass $M_A - 5\%M_A < M_{b\bar{b}} < M_A + 5\%M_A$. In $\sigma_{P_T}^{cut}$ a cut on transverse momentum of leptons $p_T > 5$ GeV is added.

M_A (GeV)	σ^{cut} (fb)	$\sigma_{P_T}^{cut}$ (fb)	σ^{cut} (fb)	$\sigma_{P_T}^{cut}$ (fb)
	$\tan\beta = 40$	$\tan\beta = 40$	$\tan\beta = 50$	$\tan\beta = 50$
150	0.240	0.124	0.660	0.340
200	0.186	0.096	0.520	0.280
300	0.122	0.074	0.340	0.172
400	0.070	0.042	0.240	0.160
500	0.052	0.024	0.148	0.076

of leptons and jets for detector acceptance and further a cut on the energy of both leptons and jets: $E > 5$ GeV; the invariant mass of the $b\bar{b}$ system is required to be in the range $M_A \pm 0.05M_A$, which is the expected experimental resolution [14]. We find that after the cuts the background processes have cross sections at the level of $10^{-3} - 10^{-4}$ fb, while the effect on the signal cross section can be read off from Table I. In particular we observe that the cut on the invariant mass $M_{b\bar{b}}$ suffices to suppress background processes. Comparing the numerical results shown in Table I (σ^{cut}) with Fig. 4 we note that the signal cross section is reduced by a factor of three; moreover we show also the effect of a supplementary cut on transverse momentum of leptons $p_T > 5$ GeV which reduces the cross section ($\sigma_{P_T}^{cut}$) by another factor of two as one might expect given the transverse momentum distributions. On the contrary, we find that the cut on the energy can be raised up to 50 GeV lowering the cross section only of $\approx 20\%$.

Another source of background are fake events where the muon comes from the decay of a τ in the lepton flavor conserving process $\gamma\gamma \rightarrow \tau^+\tau^-b\bar{b}$: this process has the same characteristic of the signal, and will pass the above cuts. The used version of COMPHEP allows the study of six particle final states, and works properly if we restrict the numbers of contributing diagram: thus we considered the dominant diagrams in $\tau\tau$ fusion with one τ decaying $\tau \rightarrow \nu\bar{\nu}\mu$. We find, without any cut, cross sections 4×10^{-2} , 2.4×10^{-2} , 6.2×10^{-3} , 7.2×10^{-4} , 2.1×10^{-5} fb for masses $M_{A,H} = 150, 200, 300, 400, 500$ GeV respectively. The suppression and the rapid fall with increasing M_A can be understood kinematically: the tree-body decay of the very energetic τ is disfavored for phase space reasons, especially at large M_A where the b are more energetic, as discussed above, and less energy is sheared by the leptons.

We finally remark that the LFV channel we are considering would naturally be a second stage study after a thorough investigation of the LFC $\tau\tau$ channel is performed, which should allow precision studies of the Higgs sector ($M_{H,A}, \tan\beta$ etc.). Thus, once the mass and other properties are known, the search for the LFV channel would be facilitated: for example, the fact that the in-

variant mass of the leptons is peaked at $2E_\gamma - M_A$ may be useful in selecting the signal (though the center of mass energy of the PC is not exactly fixed, as discussed above, at the luminosity peak the photons are almost monochromatic).

V. CORRELATIONS WITH LOW ENERGY CONSTRAINTS

The Higgs bosons LFV vertices and the branching ratios depend on the parameters of the theory (MSSM+LFV) that are subject to non-trivial constraints by experiments. In order to provide a detailed study of the possibilities of a photon collider with respect to the LFV violating signal $\gamma\gamma \rightarrow \mu\tau b\bar{b}$ we scan over the following parameter space:

$$\begin{aligned}
1 \text{ TeV} &\leq (\mu, m_{\bar{q}}, A_u, A_d, m_L, m_R) \leq 5 \text{ TeV}, \\
500 \text{ GeV} &\leq (M_1, M_2, M_3) \leq 5 \text{ TeV}, \\
150 \text{ GeV} &\leq M_A \leq 1 \text{ TeV}, \\
30 &\leq \tan\beta \leq 60, \\
10^{-3} &\leq (\delta_{LL}^{32}, \delta_{RR}^{32}) \leq 0.5.
\end{aligned} \tag{20}$$

The parameters $(\delta_{LL}^{32}, \delta_{RR}^{32})$, defined in Eq. 6, measure, in a model independent way, the amount of lepton flavor violation. We verified that δ_{LL}^{32} , which give the most important contribution, should be greater than $\simeq 5 \times 10^{-2}$ to have substantial cross section.

We impose the SUSY parameter space to respect the following constraints: lower bound on the light Higgs mass $m_h > 114.4$ GeV; upper bound on the anomaly of the muon magnetic moment $(g-2)_\mu < 5 \times 10^{-9}$; bounds on electro-weak precision observables such as $\Delta\rho < 1.5 \times 10^{-3}$; direct search constraints on the lightest chargino and sfermion masses and constrains on squarks and gluino masses from LEP and Tevatron are automatically satisfied as they lie in the TeV range in our scenario.

Some B -physics processes, namely $B_s \rightarrow \mu^+\mu^-$, $B \rightarrow X_s\gamma$ and $B_u \rightarrow \tau\nu$, are particularly sensitive to $\tan\beta$ enhanced Higgs contributions which have been subject of extensive recent studies [27, 28, 29, 31]. In particular: using the formulas for the branching ratio given

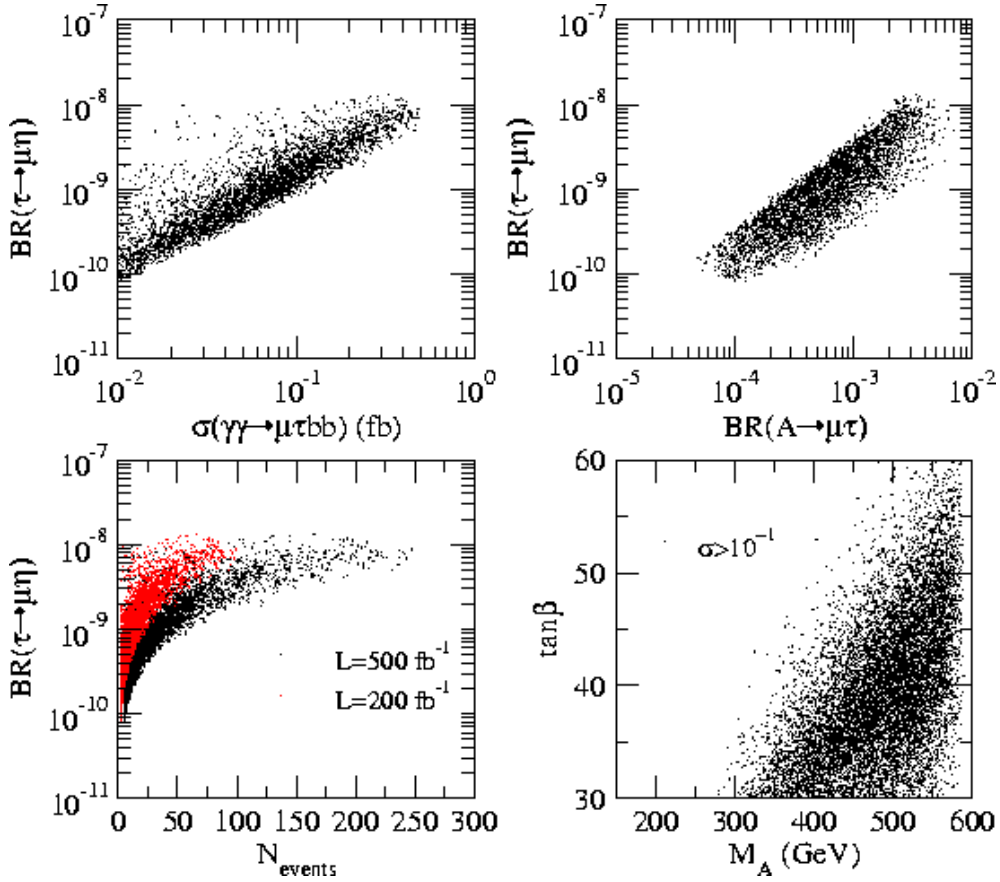


FIG. 7: (Top left panel) Correlation between $\mathcal{B}(\tau \rightarrow \mu\eta)$ and $\sigma(\gamma\gamma \rightarrow \mu\tau b\bar{b})$. (Top right panel) Correlation between $\mathcal{B}(\tau \rightarrow \mu\eta)$ and $A \rightarrow \mu\tau$. (Bottom left panel) Correlation between $\mathcal{B}(\tau \rightarrow \mu\eta)$ and the number of expected events for two values of the integrated luminosity. (Bottom right panel) Distribution of the signal cross section in the $(M_A, \tan\beta)$ plane. The parameter space and the imposed constraints are discussed in the text.

in Ref. [29] we require that the parameter space satisfies $\mathcal{B}(B_s \rightarrow \mu^+\mu^-) < 6.5 \times 10^{-8}$ [34]; $R_{\tau\nu}$, the ratio between the SUSY and SM branching ratios for $B_u \rightarrow \tau\nu$, is required in the bracket $0.70 < R_{\tau\nu} < 1.44$ using the formula in Ref. [31] and the numerical bounds from [30]; $R_{X_s\gamma}$, the ratio between the SUSY and SM branching ratios for $B \rightarrow X_s\gamma$, is required to lie in the bracket $1.01 < R_{X_s\gamma} < 1.25$ through the formulas of Ref. [27] and the numerical bounds are taken from [30].

At last, we impose the current upper bounds on LFV τ decays to be respected: $\mathcal{B}(\tau^- \rightarrow \mu^-\eta) < 6.8 \times 10^{-8}$ and $\mathcal{B}(\tau^- \rightarrow \mu^-\gamma) < 5.6 \times 10^{-8}$ [34]. In the case where Higgs-mediated LFV effects are important, $\tau \rightarrow \mu\eta$ is generally the dominant process [22, 23, 25].

We employ the analytical formulas of Section II for the cross section which gives a reasonable estimate when cuts are taken into account.

In Fig. 7, top-left panel, we show the correlation between $\mathcal{B}(\tau \rightarrow \mu\eta)$ and $\sigma(\gamma\gamma \rightarrow \mu\tau b\bar{b})$, while in the bottom-left panel, the correlation between $\mathcal{B}(\tau \rightarrow \mu\eta)$ and the numbers of $\mu\tau b\bar{b}$ events given by the previous

cross section available at a photon collider for two values of the integrated luminosity, $\mathcal{L} = 200 - 500 \text{ fb}^{-1}/\text{yr}$. It can be seen that for the high luminosity option we can expect up to 250 events per year, and up to 100/yr for the low luminosity option. The above conclusions are valid for the present upper limits on the branching ratios: if in the near future the experimental upper bound will be improved (i.e. lowered), say by an order of magnitude, only few tens of events can be expected unless higher values of luminosity should become in the meantime available.

In the bottom-right panel we show the region of the parameter space in the $(M_A, \tan\beta)$ plane which is characterized by a signal cross-section $\sigma \geq 10^{-1} \text{ fb}$. Let us remark that the signal cross-sections becomes larger at low M_A masses, see Fig. 4 and Eq. (18). However in the considered region of large $\tan\beta$ values such low masses are excluded by the imposed constraints. In particular, the LFV signal for M_A masses below 300 GeV are excluded for all values of $\tan\beta$ in the interval, $30 < \tan\beta < 60$. We have checked that requiring a signal cross section $10^{-2} \text{ fb} \leq \sigma \leq 10^{-1} \text{ fb}$ the same region in the $(M_A, \tan\beta)$ plane is covered.

Finally, in the top-right panel we show the correlation between $\mathcal{B}(\tau \rightarrow \mu\eta)$ and $\mathcal{B}(A \rightarrow \mu\tau)$. The latter gets values in the interval $(5 \times 10^{-4}) \lesssim \mathcal{B}(A \rightarrow \mu\tau) \lesssim (8 \times 10^{-3})$. Even if the upper limit on $\mathcal{B}(\tau \rightarrow \mu\eta)$ is lowered by an order of magnitude from its actual value ($\approx 10^{-8}$) we see that $\mathcal{B}(A \rightarrow \mu\tau)$ can still reach values up to $\mathcal{O}(10^{-3})$ which are particularly interesting for the LHC, where the cross section for heavy neutral gauge bosons production in $b\bar{b}$ fusion is sizable [9].

VI. SUMMARY AND CONCLUSIONS

In this work we present a detailed study of LFV signals at a photon collider, namely $\gamma\gamma \rightarrow \mu\tau b\bar{b}$, mediated by the MSSM heavy Higgs bosons (A, H). Our approach is model-independent with respect to the source of lepton flavour violation. Effective couplings of the MSSM higgs bosons which violate lepton flavor conservation arise at loop level once in the model (MSSM) it is introduced a source of LFV in the slepton mass matrix. This happens for example in the so called ν -MSSM (SUSY see-saw mechanism) where off-diagonal elements in the slepton mass matrix are induced by the running of the parameters from the heavy right-handed neutrino scale to the electroweak symmetry breaking scale.

The effects are particularly enhanced at large $\tan\beta$ and if the SUSY spectrum is beyond the TeV range LFV τ -decays like $\tau \rightarrow \mu\eta$ and $\tau \rightarrow \mu\gamma$ are pushed near the experimental upper limit and their search can be refined or expected to give a positive result both at the LHC and at a super-B factory. At the same time also lepton flavor conserving processes like the B-physics channels $B \rightarrow \mu^+\mu^-$, $B \rightarrow \tau\nu$ and $B \rightarrow X_s\gamma$ have high sensitivity to the above scenario and put severe constraints on the parameter space.

At forthcoming LHC experiments the heavy neutral Higgs bosons can be produced copiously and the decay $(A, H) \rightarrow \mu\tau$ detected [8, 9]. An analysis at the future ILC in the e^+e^- mode was carried out in Ref. [10]. In this paper we extend this analysis to explore the potential of a photon collider, which is known to be an interesting option of the ILC, in detecting LFV signal mediated by heavy neutral Higgs bosons of the MSSM. In [14] it was shown that within the considered scenario the process $\gamma\gamma \rightarrow \tau\tau b\bar{b}$ ($\tau\tau$ -fusion) is the principal mechanism for heavy Higgs production in photon-photon collisions and that it allows to measure $\tan\beta$ with a precision which is better than that obtainable at the LHC. In this work we show that in $\gamma\gamma$ collisions the dominant channel for the lepton flavor violating process $\gamma\gamma \rightarrow \mu\tau b\bar{b}$ is that

in which the colliding photons split respectively into a μ -pair and τ -pair and the two virtual leptons ($\mu\tau$) annihilate into the Higgs which decay into a $b\bar{b}$, Fig. 1(a). We give both an analytical approximation of the cross section and a detailed numerical study of the signal by evaluation of the contributing diagrams discussing background and the necessary cuts to isolate the signal. The observability of the signal has been studied by imposing on the large parameter space the constraints on the SUSY spectrum obtained by electro-weak precision observables, direct search, B physics and experimental upper bounds on the rare τ -LFV decays. We have considered as reference values of the technical parameters of the photon collider those of the TESLA project assuming an integrated luminosity $\mathcal{O}(200 - 500) \text{ fb}^{-1}/\text{yr}$ and $\sqrt{s_{\gamma\gamma}} = 600 \text{ GeV}$.

Let us finally summarize the results obtained in this work: *i*) for large values of $\tan\beta$, ($30 < \tan\beta < 60$) the cross of $\gamma\gamma \rightarrow \mu\tau b\bar{b}$ goes from 10^{-2} fb up to a few fb for higgs bosons masses ranging from $M_{A,H} > 150$ up to the kinematical limit, 600 GeV; *ii*) the heavy neutral Higgs (A, H) are practically degenerate in mass and give the same contribution to the signal cross section; *iii*) the μ and τ leptons are emitted preferentially back-to-back and are characterized by high energy and low transverse momentum. A cut on the energy up to 50 GeV can be safely applied without affecting very much the cross-section while on the contrary a cut on transverse momentum would decrease the signal cross-section drastically. The b-tagged jets from the Higgs decay have invariant mass distributions which are peaked at the Higgs mass. A cut on the invariant mass is sufficient to reduce significantly the background; *iv*) low energy constraints put further conditions on the observability of the signal: the parameter space is restricted to those regions which are allowed by the low energy constraint and there we look for points where the signal cross section are in the range $10^{-1} - 10^0 \text{ fb}$ or $\sigma > 10^{-1}$, giving up to 250 events/yr for the high luminosity option and up to 100 events/yr for the low luminosity case; *v*) once the low energy constraints are applied to the parameter space we find that the lepton flavor violating signal can be probed for masses of the heavy neutral Higgs bosons A, H from 300 GeV up to the kinematical limit $\simeq 600 \text{ GeV}$ for $30 \leq \tan\beta \leq 60$.

ACKNOWLEDGMENTS

The authors would like to acknowledge P. Paradisi for collaboration in the early stages of this work and for many useful discussions.

[1] J. Brau *et al.*, “International Linear Collider reference design report. 1: Executive summary. 2: Physics at the

ILC. 3: Accelerator. 4: Detectors.”; See also: A. Djouadi *et al.* [ILC Collaboration], “Intern-

- tional Linear Collider Reference Design Report Volume 2: PHYSICS AT THE ILC,” arXiv:0709.1893 [hep-ph].
- [2] B. Badelek *et al.* [ECFA/DESY Photon Collider Working Group], “TESLA Technical Design Report, Part VI, Chapter 1: Photon collider at TESLA,” *Int. J. Mod. Phys. A* **19**, 5097 (2004), [arXiv:hep-ex/0108012] Web page on TDR Photon Collider: <http://www.desy.de/~telnov/tdr/ggtdr.ps.gz>
- [3] I. F. Ginzburg, G. L. Kotkin, V. G. Serbo and V. I. Telnov, *Nucl. Instrum. Meth.* **205** 47 (1983); I. F. Ginzburg, G. L. Kotkin, S. L. Panfil, V. G. Serbo and V. I. Telnov, *Nucl. Instrum. Meth. A* **219** 5 (1984).
- [4] A. Djouadi, *Phys. Rept.* **459**, 1 (2008) [arXiv:hep-ph/0503173].
- [5] A. Djouadi, *Phys. Rept.* **457**, 1 (2008) [arXiv:hep-ph/0503172].
- [6] F. Borzumati and A. Masiero, *Phys. Rev. Lett.* **57**, 961 (1986).
- [7] K. S. Babu and C. Kolda, *Phys. Rev. Lett.* **89**, 241802 (2002) [arXiv:hep-ph/0206310].
- [8] A. Brignole and A. Rossi, *Phys. Lett. B* **566**, 217 (2003) [arXiv:hep-ph/0304081].
- [9] J. L. Diaz-Cruz, D. K. Ghosh and S. Moretti, arXiv:0809.5158 [hep-ph].
- [10] S. Kanemura, K. Matsuda, T. Ota, T. Shindou, E. Takasugi and K. Tsumura, *Phys. Lett. B* **599**, 83 (2004) [arXiv:hep-ph/0406316].
- [11] M. Cannoni, S. Kolb and O. Panella, *Phys. Rev. D* **68** (2003) 096002 [arXiv:hep-ph/0306170].
- [12] M. Cannoni, C. Carimalo, W. Da Silva and O. Panella, *Phys. Rev. D* **72** (2005) 115004 [Erratum-ibid. *D* **72** (2005) 119907] [arXiv:hep-ph/0508256].
- [13] M. Cannoni, C. Carimalo, W. Da Silva and O. Panella, *Acta Phys. Polon. B* **37** (2006) 1079.
- [14] S. Y. Choi, J. Kalinowski, J. S. Lee, M. M. Muhlleitner, M. Spira and P. M. Zerwas, *Phys. Lett. B* **606**, 164 (2005) [arXiv:hep-ph/0404119].
- [15] J. Hisano, T. Moroi, K. Tobe, M. Yamaguchi and T. Yanagida, *Phys. Lett. B* **357**, 579 (1995) [arXiv:hep-ph/9501407].
- [16] J. Hisano, T. Moroi, K. Tobe and M. Yamaguchi, *Phys. Rev. D* **53**, 2442 (1996) [arXiv:hep-ph/9510309].
- [17] A. Masiero, S. K. Vempati and O. Vives, *New J. Phys.* **6**, 202 (2004)
- [18] A. Masiero, S. K. Vempati and O. Vives, *Nucl. Phys. B* **649**, 189 (2003) [arXiv:hep-ph/0209303].
- [19] K. S. Babu and C. F. Kolda, *Phys. Rev. Lett.* **84**, 228 (2000) [arXiv:hep-ph/9909476].
- [20] S. Heinemeyer, W. Hollik and G. Weiglein, *Comput. Phys. Commun.* **124**, 76 (2000) [arXiv:hep-ph/9812320]; Home page: www.feynhiggs.de.
- [21] P. Paradisi, *JHEP* **0608**, 047 (2006) [arXiv:hep-ph/0601100].
- [22] P. Paradisi, *JHEP* **0602**, 050 (2006) [arXiv:hep-ph/0508054].
- [23] M. Sher, *Phys. Rev. D* **66**, 057301 (2002) [arXiv:hep-ph/0207136].
- [24] A. Dedes, J. R. Ellis and M. Raidal, *Phys. Lett. B* **549**, 159 (2002) [arXiv:hep-ph/0209207];
- [25] A. Brignole and A. Rossi, *Nucl. Phys. B* **701**, 3 (2004) arXiv:hep-ph/0404211;
- [26] J. K. Parry, *Nucl. Phys. B* **760**, 38 (2007) [arXiv:hep-ph/0510305].
- [27] G. D’Ambrosio, G. F. Giudice, G. Isidori and A. Strumia, *Nucl. Phys. B* **645**, 155 (2002) [arXiv:hep-ph/0207036];
- [28] G. Isidori and A. Retico, *JHEP* **0111**, 001 (2001) [arXiv:hep-ph/0110121];
- [29] A. J. Buras, P. H. Chankowski, J. Rosiek and L. Slawianowska, *Nucl. Phys. B* **659**, 3 (2003) [arXiv:hep-ph/0210145];
- [30] A. Masiero, P. Paradisi and R. Petronzio, arXiv:0807.4721 [hep-ph].
- [31] G. Isidori and P. Paradisi, *Phys. Lett. B* **639**, 499 (2006) [arXiv:hep-ph/0605012].
- [32] S. Kanemura, T. Ota and K. Tsumura, *Phys. Rev. D* **73**, 016006 (2006) [arXiv:hep-ph/0505191].
- [33] E. Boos *et al.* [CompHEP Collaboration], *Nucl. Instrum. Meth. A* **534**, 250 (2004) [arXiv:hep-ph/0403113]; A. Pukhov *et al.*, arXiv:hep-ph/9908288; Home page: <http://comphep.sinp.msu.ru>.
- [34] C. Amsler *et al.* [Particle Data Group], *Phys. Lett. B* **667**, 1 (2008).